Title

Structure and Candidate Biosynthetic Gene Cluster of a Manumycin-Type Metabolite from Salinispora pacifica

Journal

Journal of Natural Products, 85(4)

ISSN

0163-3864

Authors

Castro-Falcón, Gabriel

Creamer, Kaitlin E

Chase, Alexander B

et al.

Publication Date

2022-04-22

DOI

10.1021/acs.jnatprod.1c01117

HHS Public Access

Author manuscript

J Nat Prod. Author manuscript; available in PMC 2022 June 21.

Published in final edited form as:

J Nat Prod. 2022 April 22; 85(4): 980–986. doi:10.1021/acs.jnatprod.1c01117.

Structure and Candidate Biosynthetic Gene Cluster of a Manumycin-Type Metabolite from *Salinispora pacifica*

Gabriel Castro-Falcón,

Kaitlin E. Creamer,

Alexander B. Chase,

Min Cheol Kim,

Douglas Sweeney,

Evgenia Glukhov,

William Fenical,

Paul R. Jensen

Center for Marine Biotechnology and Biomedicine, Scripps Institution of Oceanography, University of California, San Diego, La Jolla, California 92093, United States

Abstract

A new manumycin-type natural product named pacificamide (**1**) and its candidate biosynthetic gene cluster (*pac*) were discovered from the marine actinobacterium *Salinispora pacifica* CNT-855. The structure of the compound was determined using NMR, electronic circular dichroism, and bioinformatic predictions. The *pac* gene cluster is unique to *S. pacifica* and found in only two of the 119 *Salinispora* genomes analyzed across nine species. Comparative analyses of biosynthetic gene clusters encoding the production of related manumycin-type compounds revealed genetic differences in accordance with the unique pacificamide structure. Further queries of manumycin-type gene clusters from public databases revealed their limited distribution across the phylum Actinobacteria and orphan diversity that suggests additional products remain to be discovered in this compound class. Production of the known metabolite triacsin D is also reported for the first time from the genus *Salinispora*. This study adds two classes of compounds to the natural product collective isolated from the genus *Salinispora*, which has proven to be a useful model for natural product research.

Graphical Abstract

Corresponding Author Paul R. Jensen – Center for Marine Biotechnology and Biomedicine, Scripps Institution of Oceanography, University of California, San Diego, La Jolla, California 92093, United States; Phone: 858-534-7322; pjensen@ucsd.edu.

Supporting Information

The Supporting Information is available free of charge at https://pubs.acs.org/doi/10.1021/acs.jnatprod.1c01117.

Detailed experimental procedures, UV/vis, ECD and MS spectra, NMR spectroscopic data, DFT models and NMR predictions, BGC annotations and comparisons, phylogenomic analysis, and cytotoxicity results (PDF)

The authors declare no competing financial interest.

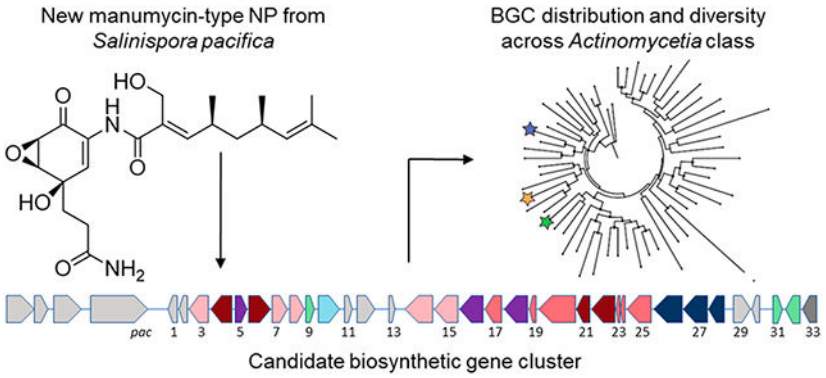

Bacterial natural products have played key roles in both the development of new drugs and the advancement of basic biomedical research.[1,2] The phylum Actinobacteria has been a particularly important source of novel natural products, with most strains originating from soils.[3] More recent explorations of marine microbes have revealed chemically rich actinobacterial lineages that are phylogenetically distinct from their terrestrial counterparts. Included among these is the marine obligate Actinobacterial genus *Salinispora*, which has proven to be a rich source of natural products with cytotoxic, antimalarial, and antibiotic activities.[4-6] The proteasome inhibitor salinosporamide A, which is currently undergoing phase III clinical trials, and the DNA intercalator lomaiviticin A are salient examples of bioactive natural products discovered from *Salinispora* species.[7,8] Our understanding of the natural product biosynthetic potential of the genus *Salinispora* has been further advanced by genome sequencing. Among 119 public genomes representing all nine named species, 305 different gene cluster families devoted to natural product biosynthesis were detected.[9-11] This figure greatly surpasses the number of natural products reported to date from *Salinispora* cultures and suggests that considerable biosynthetic potential remains to be realized.

Herein, we report the new metabolite pacificamide (**1**) from *Salinispora pacifica* CNT-855 and the known metabolite triacsin D from *Salinispora cortesiana* CNY-202. Both compounds, previously unknown from the genus, were initially targeted from a large-scale comparative metabolomics data set that included all nine *Salinispora* species.[11] We focus on the isolation, structure elucidation, and biological activity of the natural product pacificamide, a new member of the manumycin group of metabolites (Figure 1).[12] We identify a candidate pacificamide biosynthetic gene cluster, which we named *pac*, in two *S. pacifica* strains and compare them to characterized manumycin-type BGCs in *Streptomyces* and *Saccharothrix* spp. to correlate gene content with structural differences in the compounds they encode. Finally, we search *pac* homologues in publicly available bacterial genome sequences to reveal the diversity and distribution of manumycin-type BGCs that have yet to be linked to their small-molecule products.

RESULTS AND DISCUSSION

Isolation and Structure Elucidation.

HPLC-UV-MS chemical profiling of culture extracts of 30 *Salinispora* spp. led to the detection of two compounds in strains *S. pacifica* CNT-855 and *S. cortesiana* CNY-202 with UV/vis and MS spectra that differed from previously identified *Salinispora* natural products. A 6–10 L cultivation of these strains yielded organic extracts, and subsequent targeted purification via C18 reversed-phase chromatography led to the isolation of the known compound triacsin D,[13,14] from CNY-202, and a new compound named pacificamide (**1**), from CNT-855, with a molecular formula assigned as $C_{22}H_{32}N_2O_6$ based on a sodium adduct ion at *m/z* 443.2149 using HR-ESI-TOF-MS.

Spectroscopic analysis of the ^{1}H NMR data of **1** (in CD_3OD) showed signals for 27 protons, including three olefinic protons at δ_H 7.29 (H-3), 6.49 (H-3′), and 4.88 (H-7′), two oxymethine protons at δ_H 3.66 (H-5) and 3.57 (H-6), an oxymethylene proton at δ_H 4.35 (H_2-10′), three methylene groups at δ_H 2.09 (H_2-7), 2.33 (H_2-8), and 1.34 (H-5′a) and 1.24 (H-5′b), two methine protons at δ_H 2.62 (H-4′) and 2.40 (H-6′), and four methyl groups at δ_H 1.68 (H_3-9′), 1.62 (H_3-13′), 1.01 (H_3-11′), and 0.90 (H_3-12′). The HSQC spectrum showed correlations for 15 carbon signals (Figure 2a), and the HMBC spectrum showed correlations to the remaining seven carbon signals, including three carbonyl carbons at δ_C 190.0 (C-1), 178.0 (C-9), and 169.3 (C-1′), three vinyl carbons at δ_C 130.4 (C-2), 132.1 (C-2′), and 131.0 (C-8′), and an *O*-substituted sp^3 carbon at δ_C 71.4 (C-4) (Figure 2c). The COSY spectrum revealed three spin–spin coupling systems including H-9′ to H-10′, H-3 to H-5, and H-7 to H-8 (Figure 2b). The HMBC spectrum showed correlations that established the connectivity of the three spin–spin coupling systems (Figure 2c). Among observed correlations, H-3 to C-1, C-2, and C-4, H-5 to C-4, and H-6 to C-1 and C-2 suggested the 5,6-epoxy-4-hydroxycyclohex-2-en-1-one of **1**, which is characteristic of many manumycin-type natural products (Figures 1 and 2c).[11] The HMBC correlations of H_2-7 to C-3, C-4, C-5, C-8, and C-9 and H_2-8 to C-9 permitted the propionic amide to be positioned at C-4 of the epoxycyclohexenone. On the basis of the molecular formula and the chemical shift of carbonyl C-1′, we inferred that the aliphatic side chain (C-2′ to C-9′) and the epoxy-cyclohexenone connection was through an amide group. Thus, the planar structure of **1** was established as drawn in Figure 2.

The relative configuration of **1** was assigned by interpretation of ^{1}H, HETLOC and NOESY NMR experiments and DFT-molecular calculations (Figure 2d). The cyclohexenone moiety (C-4 to C-6) including a *cis* epoxide ring was defined as 4*R**, 5*S**, 6*R** due to NOESY correlations of H-3/H-7, H-3/H-8, H-5/H-6, H-5/H-7, and H-5/H-8. Consistent with this, the *syn*-configuration between 4-hydroxy and 5,6-epoxide groups is a general characteristic of all manumycin-type metabolites.[15] On the “upper” side chain of **1**, the C-2′ to C-3′ double bond was defined as *E* due to a NOESY correlation between H-4′ and H-10′. As observed by ^{1}H NMR, a large $^3J_{H,H}$ (10.3 Hz) between vinylic H-3′ and H-4′ suggested these were in *anti*-conformation, which would result in low 1,3-allylic strain. A similar relationship was observed for H-6′ and vinylic H-7′ ($^3J_{H,H}$ = 10.2 Hz). As observed by HETLOC,[16] a large $^3J_{C,H}$ (6.4 Hz) between C-3′ and H-5′a suggested their *anti*-conformation. Similarly,

C-7′ and H-5′a ($^3J_{C,H}$ = 6.8 Hz) were also in *anti*-conformation. Moreover, both C-12′ and C-11′ shared small $^3J_{C,H}$ (<4 Hz) with both H-5′a/H-5′b, suggesting their *gauche*-conformation. These results supported a conformation unique to **1** with *syn*-configured 4′*S**,6′*R**-dimethyl groups (Figure 2d). The $\Delta\delta^1$H between H-5′a and H-5′b of 0.10 ppm did not support either configuration for the 4,6-dimethyl substituents.[17] Thus, to confirm our configurational assignment, we performed DFT calculations with ^{1}H and ^{13}C NMR chemical shift predictions on *syn*- and *anti*-configured models of the "upper" side chain of **1**.[18,19] Based on the differences between the calculated and experimental chemical shifts for *syn* $\Delta\delta_{H,ave}$ = 0.051 ppm and $\Delta\delta_{C,ave}$ = 1.5 ppm) and *anti* ($\Delta\delta_{H,ave}$ = 0.091 ppm and $\Delta\delta_{C,ave}$ = 1.5 ppm) models, the *syn* model proved to be a better match to **1**. Furthermore, the structures of the lowest energy optimized conformers for the *syn* model were in agreement with the conformation observed via NMR analysis (Figure 2d).

The absolute configuration of the cyclohexenone moiety was assigned as 4*R*, 5*S*, 6*R* based on the electronic circular dichroism (ECD) spectrum of **1**, which showed a positive Cotton effect at λ_{max} ($\Delta\varepsilon$) 328 nm (+1.05) attributed to the position of the epoxide oxygen with respect to the cyclohexene chromophore in accordance with the "inverse quadrant" rule for epoxyquinols.[20-22] This assignment is consistent with the absolute configuration established for the salternamide natural products (Figure 1).[23] The absolute configuration determination for the "upper" side chain of **1** as 4′*S*,6′*R* is based on genetic evidence that follows below.

Biosynthetic Gene Cluster Analysis.

AntiSMASH analysis of the *Salinispora pacifica* CNT-855 genome (NCBI accession AZWS00000000) led to the identification of a candidate BGC for the production of **1** that shared similarity to both the asukamycin BGC (*asu*) from *Streptomyces nodosus* subsp. *asukaensis* and the colabomycin BGC (*col*) from *Streptomyces aureus*.[24-27] A query of 119 *Salinispora* genomes revealed that only one additional strain, *S. pacifica* CNS-960, possessed the candidate pacificamide BGC, which we have named *pac*. A comparison of the *pac* BGC in the two *Salinispora* strains helped to establish BGC boundaries (*pac1–33*) and identify two transposase genes in CNS-960 (between *pac12* and *−13*) as the only difference in gene content (Figure 3a). When grown under similar conditions, we observed production of **1** in CNS-960, albeit in reduced quantity relative to strain CNT-855 (Figure 3d).

The *pac* BGC shares several genes with *asu* and *col* that encode essential enzymes in the biosynthesis of their cognate small molecules and served as key references for this work.[24-26] *Pac* also shows similarity to the recently identified "compound A" BGC (*esp*) from *Saccharothrix espanaensis* DSM-44229,[28] the manumycin BGC (*man*), which we deduced from mining the manumycin A producer *Streptomyces griseoaurantiacus* M045 genome (RefSeq accession GCF_000204605.1),[29,30] and the daryamide BGC (*dar*), which we identified and named in the course of this study via genome sequencing of the daryamide and novodaryamide producer *Streptomyces* sp. CNQ-085 (NCBI accession no. JAJFAU000000000).[31,32] Key biosynthetic genes shared among these BGCs include three genes (*pac26–28*) related to the synthesis and priming of 3-amino-4-hydroxybenzoic acid (3,4-AHBA), two type II PKS genes (*pac21* and *−22*) involved in the production of polyene natural products (as classified by NaPDoS)[33] and associated with the formation of the

"lower" side chain that extends from the carbonyl of 3,4-AHBA, two KS III genes (*pac4* and *pac6*) associated with the first condensation step in the biosynthesis of the "upper" acyl chain,[34] one arylamine *N*-acyltransferase gene (*pac17*) involved in the ligation of the "upper" side chain to the amino-hydroxy phenyl moiety, three oxidoreductase genes (*pac5, pac16*, and *pac18*) responsible for the formation of the 5,6-epoxy-4-hydroxycyclohex-2-en-1-one moiety, and acyl carrier protein, acyltransferase, and thioesterase encoding genes (Figure 3 and Supporting Information, Figure S11).[24-26] A feature of the biosynthesis that remains unknown is the "upper" side chain extension following priming by the KS III. This is suspected to involve fatty acid synthases encoded in other regions of the genome.[23]

To explain the structural differences between **1** and other manumycin-type compounds, we focused on gene differences among the *pac, asu, col, esp, man*, and *dar* BGCs (Figure S11). We found a predicted enoyl-reductase (ER, *fabV* homologue) gene in the *pac* and *dar* BGCs (*pac25* and *dar7*, respectively) that could be responsible for the saturated "lower" side chain in both **1** and the daryamides. This gene is lacking in the *asu, col, man*, and *esp* BGCs, which instead yield metabolites with a polyunsaturated "lower" side chain. We expect the presence of a similar gene in the BGCs that code for U62-162 and the salternamides, which also display a saturated lower side chain (Figure 1); however genome sequences are not available. Additionally, we found an asparagine synthase gene (a homologue of *nspN* from 4-hydroxy-3-nitrosobenzamide biosynthesis)[35] in the *pac* and *dar* BGCs (*pac20* and *dar24*) that could be responsible for installing the primary amides on the "lower" side chains of **1** and the daryamides. This gene is absent in the *asu, col, man*, and *esp* BGCs, which instead share three genes encoding the synthesis and ligation of the 2-amino-3-hydroxycyclopente-2-one ring observed in many manumycin-type metabolites.[24-26,36] Finally, we found a cytochrome P450 gene (*pac15*) that is not observed in the other manumycin-type BGCs and could be responsible for installing the hydroxymethylene of **1**, which is a unique feature within the manumycin natural product family.

It is noteworthy that the *pac* BGC lacks the ketoreductase gene (KR, FabG homologue) and two dehydratase genes (DH, MaoC homologues) shared among all other manumycin-type BGCs (e.g., *asuC7–C9* and *dar1,18,19* in Figure 3a). These activities are expected during polyketide extension cycles to achieve the "upper" and "lower" side chains of **1**. Alternatively, we propose that *pac7*, which encodes a dehydrogenase (FadB homologue with documented ketoreduction activity[37]), is responsible for beta-ketoreduction and that *pac8*, which encodes for an enoyl hydratase/isomerase of the crotonase family, is responsible for the predicted dehydration steps, as has been previously observed.[38] During the initial extension leading to the "upper" side chain, we propose that *pac8* is also responsible for a 2-enoyl to 3-enoyl alkene shift resulting in the C-7′/C-8′ alkene in **1**. Another gene of interest is *pac33*, encoding a DsbA family oxidoreductase. While the role of this gene in the *pac* BGC is not known, some manumycins disrupt the mammalian DsbA-DsbB complex through direct covalent modification.[39] Thus, *pac33* may encode a resistant version of this target, as we have previously observed for a *fabB* homologue and the fatty acid inhibitor thiolactomycin.[40]

Next, we asked if bioinformatic analysis of key biosynthetic genes could facilitate prediction of the absolute configuration of **1**. Apart from the suspected involvement in "lower" side chain saturation, the *pac25* enoyl-reductase (FabV homologue) could also be responsible for the saturation on the "upper" side chain and, thus, instrumental in determining the configuration of the 4′ position. The stereospecificity of prokaryotic fatty acid enoyl-reductases reveals that protonation on the enolate intermediate occurs on the 2-*re* face.[41 43] Following this logic, **1** is predicted to have a 4′*S* and 6′*R* absolute configuration, which agrees with the configuration of the salternamides as assigned on the basis of ECD spectroscopy in combination with DFT calculations.[23]

Manumycin-Type BGC Diversity and Distribution.

To gain insight into the broader diversity of manumycin-type BGCs, we queried *pac* against the NCBI reference sequence (refseq), nonredundant (nr), metagenomic (env_nr), and patented (pataa) protein databases and the MIBiG 2.0 BGC database using cblaster.[44] This analysis identified 29 manumycin-type BGCs in addition to the seven already mentioned (Figure 4). Hierarchical clustering based on best hit identity values[44] combined with manual comparison between the top cluster matches revealed 11 groups of closely related BGCs, six of which have been linked to specific manumycin-type metabolites (Figure 4). The remaining five BGC groups have unique organizations suggesting additional diversity remains to be discovered in this compound class. When placed in a phylogenomic context, the 36 BGCs are observed in three evolutionary distant families (*Micromonosporaceae, Streptomycetaceae*, and *Pseudonocardiaceae*) within the class Actinomycetia, suggesting they have been subject to horizontal gene transfer (Figure S12).

Biological Activities.

Pacificamide and triacsin D were tested for antibacterial activity against *Escherichia coli* MG1655 and *Bacillus oceanisediminis* CNY-977 and for cytotoxic activity against the NCI-H460 lung cancer cell line. Pacificamide showed weak activity against *B. oceanisediminis* (MIC of 50 μM), while triacsin D was cytotoxic against the lung cancer cell line (EC_{50} of 5.5 ± 0.9 μM, Figure S15).

In conclusion, we report a new manumycin-type natural product from the marine actinomycete *Salinispora pacifica* along with its candidate biosynthetic gene cluster. The candidate BGC was compared to those reported for related compounds to explore the relationships between genetic and structural diversity. This BGC class is rare among sequenced genomes, and yet-to-be-characterized variants suggest that additional structural diversity remains to be discovered. Furthermore, this study confirms production of a natural product in the triacsin family from *Salinispora* spp., which was previously predicted based on genome mining.[45]

EXPERIMENTAL SECTION

General Experimental Procedures.

Optical rotations were recorded on a Jasco P-2000 polarimeter. UV spectra were measured on a Beckman-Coulter DU800 spectrophotometer. ECD spectra were measured on a Jasco

J-810 spectropolarimeter. IR spectra were acquired on a JASCO FTIR-4100 spectrometer. 1D and 2D NMR spectroscopic data were obtained on a JEOL 500 MHz or a Bruker 600 MHz NMR spectrometer. NMR chemical shifts were referenced to the residual solvent peaks (δ_H 3.31 and δ_C 49.15 for CD_3OD). High-resolution ESI-TOF mass spectrometric data were acquired on an Agilent 6530 Accurate-Mass Q-TOF mass spectrometer coupled to an Agilent 1260 LC system.

Cultivation of *Salinispora pacifica* CNT-855.

A frozen stock of *S. pacifica* CNT-855 was inoculated into 50 mL of medium A1FBC [1% potato starch, 0.4% yeast extract, 0.2% peptone, 0.1% calcium carbonate, 0.01% potassium bromide, 0.04% iron sulfate (pentahydrate), and 2.2% InstantOcean in DI H_2O]. The seed culture was shaken at 200 rpm and 28 °C for 7 days and used to inoculate 1 L of medium A1FBC in a 2.8 L Fernbach flask. This culture was similarly shaken at 200 rpm and 28 °C for 7 days, after which 15 mL was inoculated into each of 10 × 2.8 L Fernbach flasks containing 1 L of medium A1FBC. After 4 days of shaking at 200 rpm and 28 °C, 25 g of sterile XAD-7 adsorbent resin was added to each flask. After three additional days of cultivation, the cultures were filtered through cheesecloth, the cells and resin were extracted with acetone (1 L) for 4 h, the extract was filtered through a cotton plug, and the acetone was removed via rotatory evaporation. The resulting extract was partitioned in a separatory funnel between EtOAc and H_2O (1:1 mixture, 600 mL total) and the organic phase collected, dried over anhydrous sodium sulfate, and concentrated via rotatory evaporation. Using this approach, it was not possible to determine if the compounds were localized to the cells, filtrate, or associated with both.

Purification of Pacificamide.

The extract (260 mg) was suspended in EtOAc, mixed with diatomaceous earth, and concentrated via rotatory evaporation to yield a powder that was dried under high-vacuum pump. The powder was loaded into a C18 reversed-phase silica gel column (4 g) that had been equilibrated with H_2O (0.1% TFA). A six-step gradient from 100% H_2O (0.1% TFA) to 100% MeCN (0.1% TFA) was used to create six fractions of differing polarity. Fraction 3 contained pacificamide and was concentrated via rotatory evaporation and lyophilization to give a brown crude (40 mg), which was further separated by HPLC [mobile phase: 38% MeCN in H_2O (0.1% TFA); stationary phase: 5 μm, C8(2), 100 Å, 250 × 10 mm (Phenomenex, Luna) column] to yield pacificamide (t_R 24 min, 4.0 mg).

Pacificamide (1): clear film; $[\alpha]_D^{22}$ + 54 (*c* 0.17, MeOH); UV/vis (MeOH) λ_{max} (log ε) 232 (3.37), 280 (3.10) nm; ECD (2.4 mM, MeOH) λ_{max} ($\Delta\varepsilon$) 210 (+1.17), 328 nm (+1.05); IR (ZnSe) ν_{max} 3330, 1662, 1628, 1047, 1024 cm^{-1}; ^1H and 2D NMR, Table S1; HR-ESI-TOF-MS *m/z* 443.2149 (calcd for $C_{22}H_{32}N_2O_6Na$, 443.2158).

BGC Bioinformatic Analyses.

Salinispora pacifica CNT-855 (IMG genome ID 2515154128) and *Salinispora pacifica* CNS-960 (dSM 45544, IMG genome ID 2517287019) were analyzed with antiSMASH 6.0 [27] with detection strictness set to “loose”. BGCs similar to *pac* were searched using

the *pac1–33* protein sequences against the NCBI reference (refseq), nonredundant (nr), metagenomic (env_nr), and patented (pataa) protein sequence databases using cblaster[44] with the following parameters: 500 BLASTp hits per query with a maximum 10 000 hits per search and 3 hits required to define a cluster, a maximum 0.01 E-value, minimum 20% identity (30% for refseq), minimum 45% query coverage for a BLASTp hit, and a maximum 20 000 bp distance from the cluster start/end and between intermediate gene hits. The *pac* BGC was queried against the MIBiG 2.0 repository using the same cblaster settings except a maximum 10 000 bp distance from start/end of a cluster to an intermediate gene. Queries resulted in 1518 clusters. The clusters were filtered to remove duplicates, ranked by cblaster cluster score, ordered by the best hit identity values using hierarchical clustering, and manually filtered for genes characteristic of manumycin-type BGCs.

Supplementary Material

Refer to Web version on PubMed Central for supplementary material.

ACKNOWLEDGMENTS

This work was supported by the National Institutes of Health (R01GM085770) to P.R.J. including diversity supplement funds to G.C.F. We are grateful to the San Diego IRACDA postdoctoral program for funding to G.C.F. and the National Science Foundation Graduate Research Fellowship Program (under grant no. DGE-1650112) to K.E.C. We thank D. Fishman and J. Granger-Jones from Laser Spectroscopy Laboratories at UC Irvine for ECD measurements, T. Molinski and M. Salib from UCSD Chemistry and Biochemistry Department for access to IR measurements, B. Duggan from the UCSD SSPPS NMR Facility for assistance with NMR experiments, and Y. Su from the UCSD Molecular Mass Spectrometry Facility for HRMS measurements. A high-resolution LC-MS instrument was provided by the National Institutes of Health (S10 OD0106400).

REFERENCES

(1). Carlson EE ACS Chem. Biol 2010, 5 (7), 639–653. [PubMed: 20509672]

(2). Newman DJ; Cragg GM J. Nat. Prod 2020, 83 (3), 770–803. [PubMed: 32162523]

(3). Katz L; Baltz RH J. Ind. Microbiol Biotechnol 2016, 43 (2–3), 155–176. [PubMed: 26739136]

(4). Mincer TJ; Jensen PR; Kauffman CA; Fenical W Appl. Environ. Microbiol 2002, 68 (10), 5005–5011. [PubMed: 12324350]

(5). Maldonado LA; Fenical W; Jensen PR; et al. Int. J. Syst. Evol Microbiol 2005, 55 (5), 1759–1766. [PubMed: 16166663]

(6). Jensen PR; Moore BS; Fenical W Nat. Prod Rep 2015, 32 (5), 738–751. [PubMed: 25730728]

(7). Feling RH; Buchanan GO; Mincer TJ; Kauffman CA; Jensen PR; Fenical W Angew. Chemie Int. Ed 2003, 42 (3), 355–357.

(8). Kim LJ; Xue M; Li X; et al. J. Am. Chem. Soc 2021, 143 (17), 6578–6585. [PubMed: 33900077]

(9). Millán-Aguiñaga N; Chavarria KL; Ugalde JA; Letzel A-C; Rouse GW; Jensen PR Sci. Rep 2017, 7 (1), 3564. [PubMed: 28620214]

(10). Román-Ponce B; Millán-Aguiñaga N; Guillen-Matus D; et al. Int. J. Syst. Evol Microbiol 2020, 70 (8), 4668–4682. [PubMed: 32701422]

(11). Chase AB; Sweeney D; Muskat MN; Guillén-Matus DG; Jensen PR MBio. 2021, 12 (6), No. e02361.

(12). Sattler I; Thiericke R; Zeeck A Nat. Prod Rep 1998, 15 (3), 221–240. [PubMed: 9652122]

(13). Tanaka H; Yoshida K; Itoh Y; Imanaka HJ Antibiot (Tokyo). 1982, 35 (2), 157–163.

(14). Omura S; Tomoda H; Xu QM; Takahashi Y; Iwai YJ Antibiot (Tokyo). 1986, 39 (9), 1211–1218.

(15). Alcaraz L; Macdonald G; Ragot JP; Lewis N; Taylor RJ K. J. Org. Chem 1998, 63 (11), 3526–3527.

(16). Matsumori N; Kaneno D; Murata M; Nakamura H; Tachibana KJ Org. Chem 1999, 64 (3), 866–876.
(17). Schmidt Y; Breit B Org. Lett 2010, 12 (10), 2218–2221. [PubMed: 20337421]
(18). Willoughby PH; Jansma MJ; Hoye TR Nat. Protoc 2020, 15 (7), 2277. [PubMed: 31949288]
(19). Willoughby P; Reisbick S Protoc. Exch 2021, DOI:10.21203/rs.2.1186/v2.
(20). Shen B; Whittle YG; Gould SJ; Keszler DA J. Org. Chem 1990, 55 (14), 4422–4426.
(21). Mohamed IE; Gross H; Pontius A; et al. Org. Lett 2009, 11 (21), 5014–5017. [PubMed: 19813715]
(22). Fu P; La S; MacMillan JB J. Nat. Prod 2017, 80 (4), 1096–1101. [PubMed: 28225277]
(23). Kim S-H; Shin Y; Lee S-H; et al. J. Nat. Prod 2015, 78 (4), 836–843. [PubMed: 25700232]
(24). Rui Z; Petříčková K; Škanta F; et al. J. Biol. Chem 2010, 285 (32), 24915–24924. [PubMed: 20522559]
(25). Rui Z; Sandy M; Jung B; Zhang W Chem. Biol 2013, 20 (7), 879–887. [PubMed: 23890006]
(26). Petříčková K; Pospíšil S; Kuzma M; et al. ChemBioChem. 2014, 15 (9), 1334–1345. [PubMed: 24838618]
(27). Blin K; Shaw S; Kloosterman AM; et al. Nucleic Acids Res. 2021, 49 (W1), W29–W35. [PubMed: 33978755]
(28). Gorniaková D; Petříček M; Kahoun D; et al. Microorganisms. 2021, 9 (3), 559. [PubMed: 33800500]
(29). Li F; Maskey RP; Qin S; et al. J. Nat. Prod 2005, 68 (3), 349–353. [PubMed: 15787434]
(30). Li F; Jiang P; Zheng H; et al. J. Bacteriol 2011, 193 (13), 3417–3418. [PubMed: 21551298]
(31). Asolkar RN; Jensen PR; Kauffman CA; Fenical WJ Nat. Prod 2006, 69 (12), 1756–1759.
(32). Castro-Falcón G; Millán-Aguiñaga N; Roullier C; Jensen PR; Hughes CC ACS Chem. Biol 2018, 13 (11), 3097–3106. [PubMed: 30272441]
(33). Ziemert N; Podell S; Penn K; Badger JH; Allen E; Jensen PR PLoS One. 2012, 7 (3), No. e34064. [PubMed: 22479523]
(34). Nofiani R; Philmus B; Nindita Y; Mahmud T Medchemcomm. 2019, 10 (9), 1517–1530. [PubMed: 31673313]
(35). Noguchi A; Kitamura T; Onaka H; Horinouchi S; Ohnishi Y Nat. Chem. Biol 2010, 6 (9), 641–643. [PubMed: 20676084]
(36). Zhang W; Bolla ML; Kahne D; Walsh CT J. Am. Chem. Soc 2010, 132 (18), 6402–6411. [PubMed: 20394362]
(37). Volodina E; Steinbüchel A AMB Express. 2014, 4 (1), 69. [PubMed: 25401070]
(38). Hamed RB; Batchelar ET; Clifton IJ; Schofield CJ Cell. Mol. Life Sci 2008, 65 (16), 2507–2527. [PubMed: 18470480]
(39). Tuladhar A; Rein KS ACS Med. Chem. Lett 2018, 9 (4), 318–322. [PubMed: 29670693]
(40). Tang X; Li J; Millán-Aguiñaga N; et al. ACS Chem. Biol 2015, 10 (12), 2841–2849. [PubMed: 26458099]
(41). Saito K; Kawaguchi A; Seyama Y; Yamakawa T; Oduda S Eur. J. Biochem 1981, 116 (3), 581–586. [PubMed: 7021150]
(42). Hu K; Zhao M; Zhang T; et al. Biochem. J 2013, 449 (1), 79–89. [PubMed: 23050861]
(43). Schiebel J; Chang A; Merget B; et al. Biochemistry. 2015, 54 (10), 1943–1955. [PubMed: 25706582]
(44). Gilchrist CLM; Booth TJ; van Wersch B; van Grieken L; Medema MH; Chooi Y-H Bioinforma Adv. 2021, vbab016, DOI: 10.1093/bioadv/vbab016.
(45). Twigg FF; Cai W; Huang W; et al. ChemBioChem. 2019, 20 (9), 1145–1149. [PubMed: 30589194]

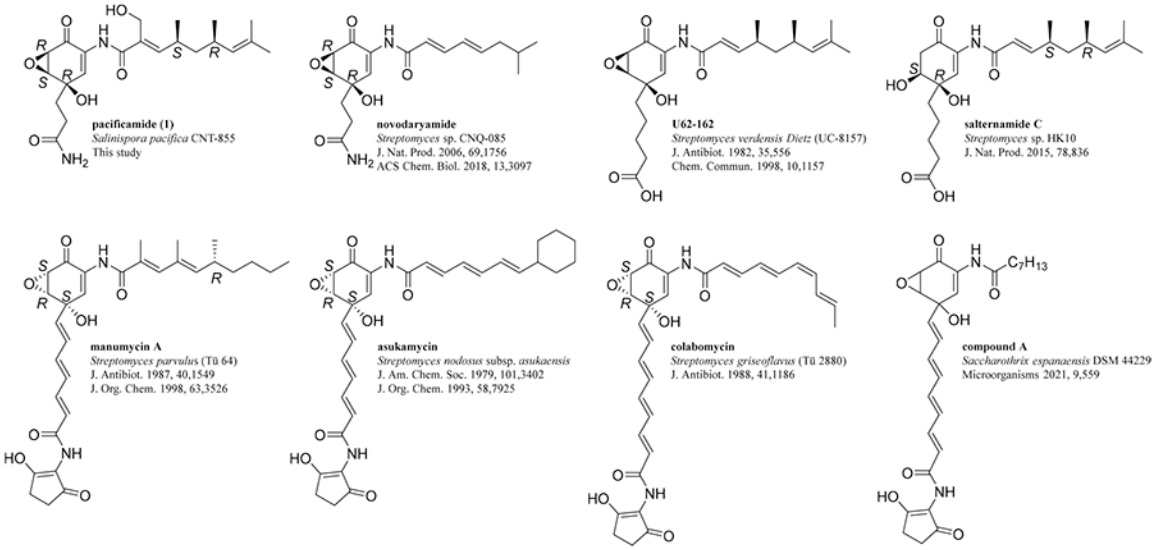

Figure 1.
Representative manumycin-type natural products.

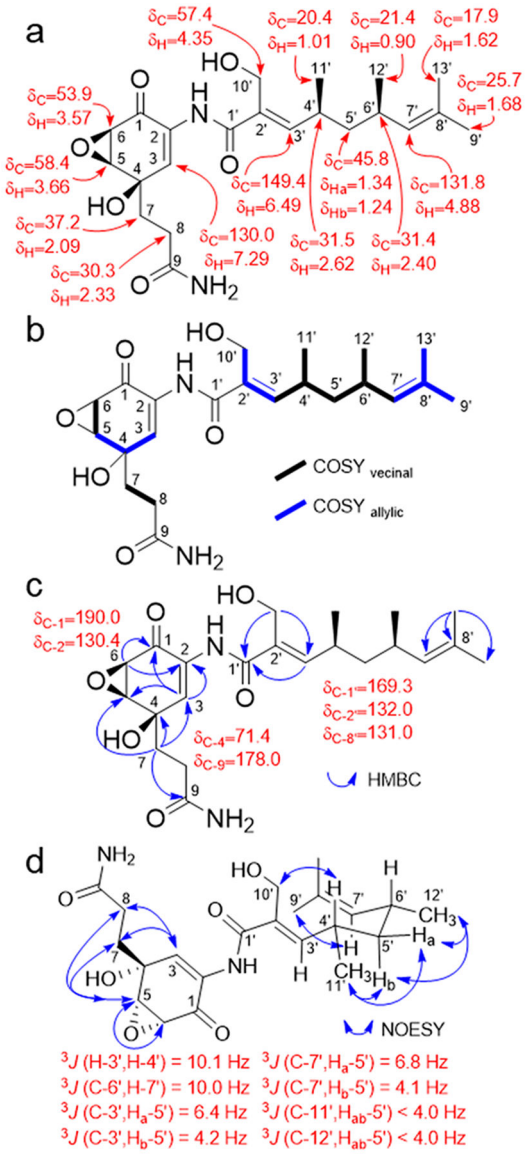

Figure 2.

NMR assignments of pacificamide (**1**). (a) ^{1}H and ^{13}C chemicals shifts (in ppm) based on ^{1}H NMR and HSQC data. (b) Spin systems observed by COSY. (c) ^{13}C chemical shifts (in ppm) and key correlations observed by HMBC. (d) Key NOESY correlations and key spin–spin coupling constants (^{3}J) observed by ^{1}H NMR and HETLOC.

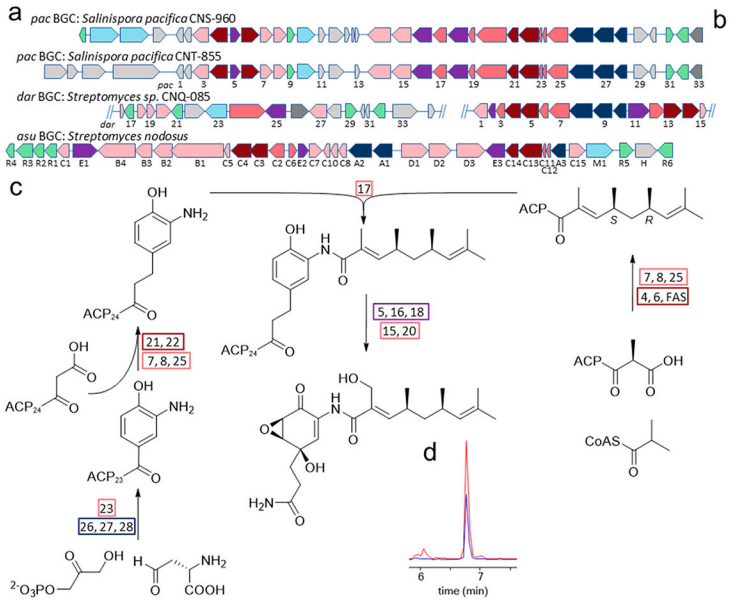

#	Predicted function	*asu* homolog	*dar* homolog
1	condensation domain of NRPS		
2	N-acetyltransferase		
3	Zn-dependent alcohol dehydrogenase		
4	beta-ketoacyl-ACP synthase III	*asuC4*	*dar14*
5	flavin reductase	*asuE2*	*dar2*
6	beta-ketoacyl-ACP synthase III	*asuC3*	*dar13*
7	3-hydroxyacyl-CoA dehydrogenase, FadB		
8	enoyl-CoA hydratase/isomerase		
9	transcriptional regulator, MerR		
10	arabinose efflux pump, MFS		*dar23*
11	reverse transcriptase/maturase-like		
12	transposase, IS110		
13	transposase, mutator		
14	acyltransferase		
15	cytochrome P450 hydroxylase		
16	flavin-dependent oxidoreductase, epoxidase	*asuE3*	*dar25*
17	arylamine N-acyltransferase	*asuC2*	*dar12*
18	flavin-dependent oxidoreductase, hydroxylase	*asuE1*	*dar11*
19	thioesterase	*asuC6*	*dar3*
20	asparagine synthetase		*dar24*
21	beta-ketoacyl-ACP synthase II (CLF)	*asuC14*	*dar4*
22	beta-ketoacyl-ACP synthase III (alpha unit)	*asuC13*	*dar5*
23	acyl carrier protein	*asuC12*	*dar6*
24	acyl carrier protein	*asuC11*	
25	enoyl-ACP reductase, FabV		*dar7*
26	AMP-dependent synthetase and ligase	*asuA2*	*dar8*
27	3-amino-4-hydroxybenzoic acid synthase	*asuA1*	*dar9*
28	2-amino-4, 5-dihydroxy-6-oxo-7-(phosphonooxy) heptanoate synthase	*asuA3*	*dar10*
29	transposase		
30	transposase		
31	transcriptional regulator		
32	transcriptional regulator		
33	DsbA family oxidoreductase		*dar26*

Figure 3.

Pacificamide BGC and biosynthesis. (a) Candidate pacificamide (*pac*) and daryamide (*dar*, two contigs) BGCs. Asukamycin (*asu*) BGC is shown for reference. Gene numbering for *pac* in CNT-855, *dar*, and *asu* is shown. Genes are color-coded by function [wine: ketosynthases; navy blue: 3,4-AHBA synthesis; purple: oxidoreductases in epoxyquinol synthesis; salmon: biosynthetic (shared); light salmon: biosynthetic (not shared); light green: regulation; light blue: transport; gray: other]. (b) *pac* gene annotations with *asu* and *dar* homologues. (c) Proposed pacificamide biosynthetic pathway (numbers represent *pac* genes). (d) LCMS extracted ion chromatogram (EIC) for pacificamide $[M + Na]^+$ from strains CNT-855 (red) and CNS-960 (blue).

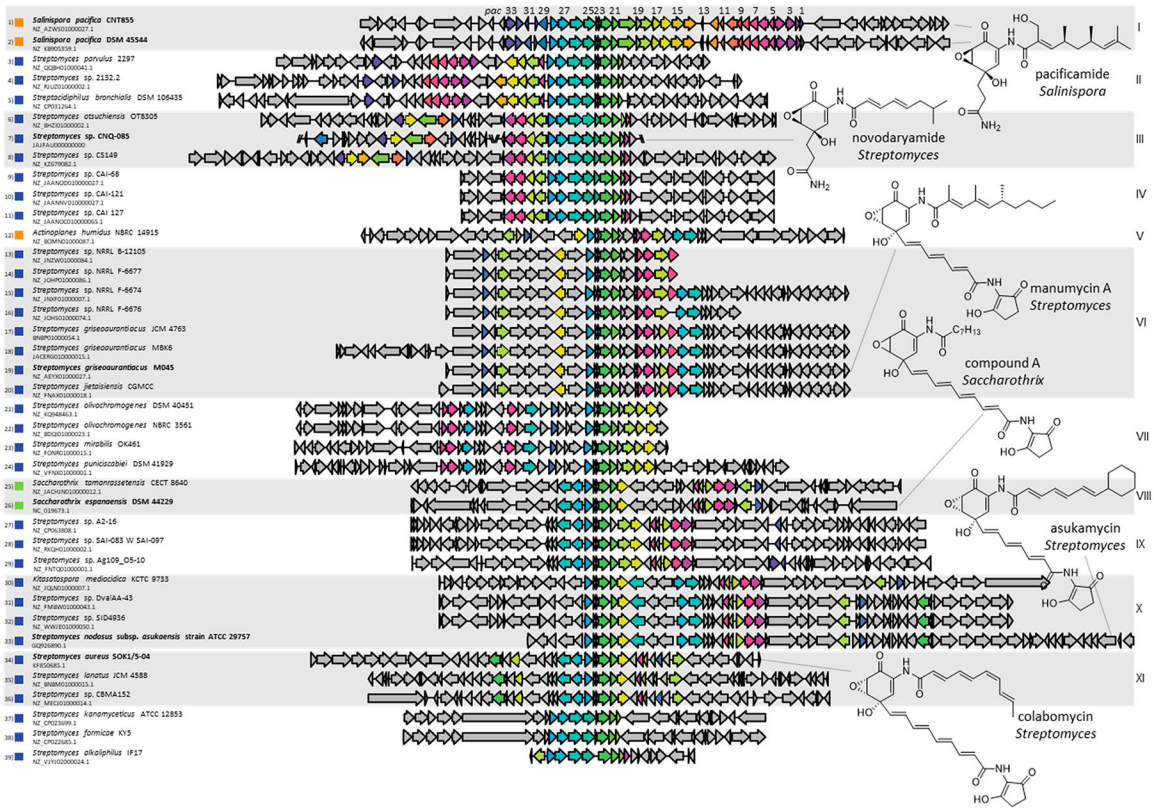

Figure 4.

Manumycin-type BGCs identified in bacterial genome sequences. Colored genes represent *pac* gene homologues. Related groups of BGCs (I–XI) are shaded gray if they have been linked to a known metabolite or unshaded if they remain orphan (entries 37–39 are not predicted to encode manumycin-type metabolites). Structures linked to the *pac, dar, man, esp, asu*, and *col* BGCs are shown with the source species in bold. Colored squares indicate family level taxa (orange: *Micromonosporaceae*, blue: *Streptomycetaceae*, and green: *Pseudonocardiaceae*).